PASylation of IL-1 receptor antagonist (IL-1Ra) retains IL-1 blockade and extends its duration in mouse urate crystal-induced peritonitis

Received for publication, August 2, 2019, and in revised form, November 11, 2019 Published, Papers in Press, December 9, 2019, DOI 10.1074/jbc.RA119.010340

Nicholas E. Powers[‡1,2], Benjamin Swartzwelter[‡3], Carlo Marchetti[‡], Dennis M. de Graaf[‡§], Alexandra Lerchner[¶], Martin Schlapschy[‖], Rajiv Datar[**], Uli Binder[¶], Carl K. Edwards III[**], Arne Skerra[‖], and Charles A. Dinarello[‡§]

*From the [‡]Department of Medicine, University of Colorado, Aurora, Colorado 80045, the [§]Department of Internal Medicine, Radboud University Medical Center, Geert Grooteplein Zuid 10, 6525 GA Nijmegen, The Netherlands, the [¶]XL-protein GmbH, Lise-Meitner-Strasse 30, 85354 Freising, Germany, the [‖]Lehrstuhl für Biologische Chemie, Technische Universität München, Emil-Erlenmeyer-Forum 5, 85354 Freising, Germany, and **DNX Biopharmaceuticals, Inc., San Diego, California 92121*

Edited by Luke O'Neill

Interleukin-1 (IL-1) is a key mediator of inflammation and immunity. Naturally-occurring IL-1 receptor antagonist (IL-1Ra) binds and blocks the IL-1 receptor-1 (IL-1R1), preventing signaling. Anakinra, a recombinant form of IL-1Ra, is used to treat a spectrum of inflammatory diseases. However, anakinra is rapidly cleared from the body and requires daily administration. To create a longer-lasting alternative, PASylated IL-1Ra (PAS–IL-1Ra) has been generated by in-frame fusion of a long, defined-length, N-terminal Pro/Ala/Ser (PAS) random-coil polypeptide with IL-1Ra. Here, we compared the efficacy of two PAS–IL-1Ra molecules, PAS600–IL-1Ra and PAS800–IL-1Ra (carrying 600 and 800 PAS residues, respectively), with that of anakinra in mice. PAS600–IL-1Ra displayed markedly extended blood plasma levels 3 days post-administration, whereas anakinra was undetectable after 24 h. We also studied PAS600–IL-1Ra and PAS800–IL-1Ra for efficacy in monosodium urate (MSU) crystal-induced peritonitis. 5 days post-administration, PAS800–IL-1Ra significantly reduced leukocyte influx and inflammatory markers in MSU-induced peritonitis, whereas equimolar anakinra administered 24 h before MSU challenge was ineffective. The 6-h pretreatment with equimolar anakinra or PAS800–IL-1Ra before MSU challenge similarly reduced inflammatory markers. In cultured A549 lung carcinoma cells, anakinra, PAS600–IL-1Ra, and PAS800-IL-Ra reduced IL-1α–induced IL-6 and IL-8 levels with comparable potency. In human peripheral blood mononuclear cells, these molecules suppressed *Candida albicans*–induced production of the cancer-promoting cytokine IL-22. Surface plasmon resonance analyses revealed significant binding between PAS–IL-1Ra and IL-1R1, although with a slightly lower affinity than anakinra. These results validate PAS–IL-1Ra as an active IL-1 antagonist with marked *in vivo* potency and a significantly extended half-life compared with anakinra.

Interleukin (IL)[3]-1α and IL-1β are initiators and regulators of innate and acquired immunity (1, 2), sterile inflammation, tissue remodeling (3), cell death (4), hypoxia-ischemia (5), and organ failure (6). First separately identified in 1974 (7), IL-1α and IL-1β signaling has since been implicated in a wide range of pathological conditions, including gout and rheumatoid arthritis (RA) (8), type II diabetes (9), and systemic autoinflammatory conditions such as cryopyrin-associated periodic syndromes (10), heart disease (11), and cancer (1).

The binding of IL-1α or IL-1β to the extracellular domain of the IL-1 receptor 1 (IL-1R1) allows the receptor to associate with the IL-1R1 accessory protein (IL-1RAcP, now IL-1R3) co-receptor, resulting in dimerization of the cytosolic Toll/interleukin-1 receptor (TIR) domains, and subsequent downstream mitogen-activated protein kinase activation as well as NF-κB nuclear translocation (12). In the nucleus, NF-κB induces transcription of inflammatory factors such as monocyte chemoattractant protein-1, IL-6, IL-8, granulocyte colony-stimulating factor (G-CSF), cyclooxygenase-2, and IL-1α and IL-1β themselves, among others (13).

The physiological and pathological activities of IL-1 are regulated by the endogenous IL-1 receptor antagonist (IL-1Ra), a member of the IL-1 family (14). IL-1Ra binds IL-1R1 with an affinity higher than IL-1α and IL-1β, but does not recruit IL-1R3, thus preventing association of TIR domains and intra-

This work was supported by National Institutes of Health Grant AI015614 (to C. A. D.), the Interleukin Foundation (to N. E. P.), and by DNX Biopharmaceuticals, Inc., San Diego, CA. C. K. E., III, and R. D. are shareholders in DNX Biopharmaceuticals, Inc., and A. S., M. S., and U. B. are shareholders of XL-protein GmbH. The content is solely the responsibility of the authors and does not necessarily represent the official views of the National Institutes of Health.

This article contains Figs. S1–S6, supporting Experimental Methods and supporting Refs. 1–5.

[1] To whom correspondence should be addressed: Dept. of Medicine, Rm. 10480A, University of Colorado Anschutz Medical Campus, 12700 East 17 Ave., Aurora, CO 80045. Tel.: 970-372-9697; E-mail: nicholas.e.powers@CUAnschutz.edu.

[2] Present address: Institute of Protein Biochemistry, National Research Council, 80131 Naples, Italy.

[3] The abbreviations used are: IL, interleukin; RA, rheumatoid arthritis; TIR, Toll/interleukin-1 receptor; G-CSF, granulocyte colony-stimulating factor; KC, keratinocyte chemoattractant; DIRA, deficiency of the interleukin-1 antagonist; IL-1Ra, IL-1 receptor antagonist; PAS, Pro/Ala/Ser polypeptide; MSU, monosodium urate; MPO, myeloperoxidase; i.p., intraperitoneal; WBC, white blood cell; FCS, fetal calf serum; ELISA, enzyme-linked immunosorbent assay; PBMC, peripheral blood mononuclear cell; RU, resonance unit; aa, amino acid; SPR, surface plasmon resonance.

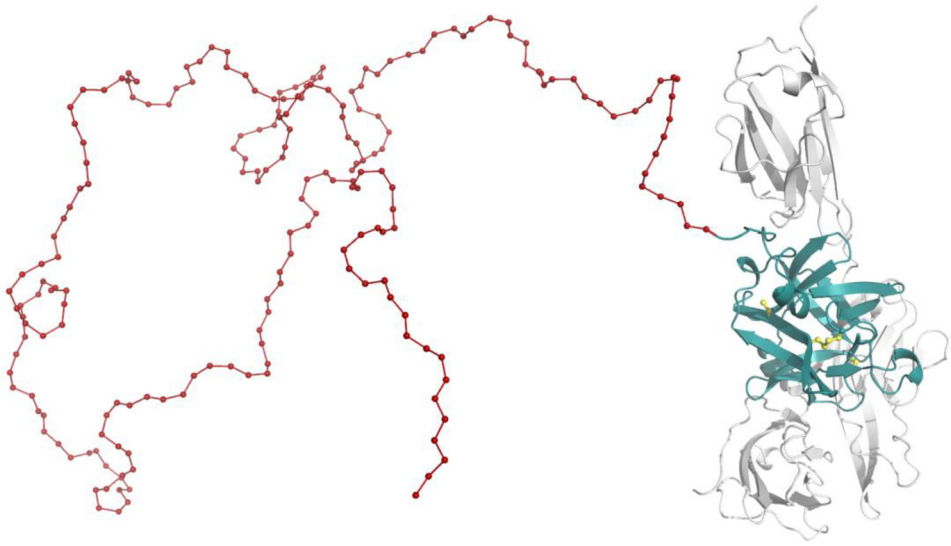

Figure 1. Three-dimensional structure of PASylated IL-1Ra. Molecular model of IL-1Ra (*teal*) with an N-terminal PAS extension (here, 200 residues, *red*) in arbitrary random conformation. Association with the extracellular domain of IL-1R1 (*gray*) is indicated (based on the crystal structure of the complex, PDB code 1IRA (67)). The four Cys side chains of IL-1Ra are highlighted (*yellow*); two of them are engaged in a structural disulfide bridge.

cellular signaling (2). The vital role of IL-1Ra in the regulation of IL-1 signaling is demonstrated in the rare genetic condition "deficiency of the interleukin-1 antagonist" (DIRA), which is associated with neonatal-onset pustular dermatosis, sterile multifocal osteomyelitis, and periostitis (15). DIRA is an autosomal recessive autoinflammatory syndrome resulting from mutations in *IL1RN*, the gene encoding IL-1Ra. Furthermore, unbalanced ratios between IL-1 and IL-1Ra occur in several models of inflammatory disease (16).

The ability of IL-1Ra to inhibit IL-1α and IL-1β signaling promoted the development of a recombinant form for therapeutic use. In 2001, anakinra (brand name Kineret®), the recombinant unglycosylated form of IL-1Ra, was approved for the treatment of RA in the United States (17–19). Since then, anakinra has been used to treat adult-onset Still's disease (20), systemic juvenile idiopathic arthritis (21), and both gout and calcium pyrophosphate deposition disease (formally pseudogout) (22). Anakinra is typically self-administered by patients via subcutaneous injection (23). Because of its small size (17.3 kDa), anakinra is rapidly removed from the body by renal filtration; a 2 mg/kg anakinra bolus has a half-life of 3.29 h in humans (24) and, notably, just a few minutes in mice (25). Anakinra requires daily administration for therapeutic effect, which poses challenges for some patients. The current need for everyday self-injection risks decreased patient treatment compliance (26). Increasing the half-life of anakinra through modification of the molecule is a new approach to address these challenges.

PASylation® is a protein modification technology first described by Schlapschy *et al.* (27) that has been used to generate several cytokines and therapeutic "biobetters" with expanded hydrodynamic volumes and half-lives, including human growth hormone (28), interferon-α (29), leptin (30), Coversin (a C5 complement inhibitor) (31), an IFN-α superagonist (32), and radiolabeled Fab fragments targeting HER2 and CD20 (33). Expression of a modified structural gene encoding a long N- or C-terminal sequence of proline, alanine, and serine residues (hence "PAS") creates a random coil chain associated with increased hydrodynamic volume without unfavorable adverse effects on the biochemical protein function (34). Importantly, immunogenicity has not been observed for any PASylated proteins tested *in vivo* in preclinical models (35, 36). Generating these fusion proteins via transcription/translation of a recombinant gene in a suitable host cell avoids challenges posed by post-translational protein modification strategies like PEGylation, including low functional yields, enhanced hydrophobicity and concerns of immunogenicity, indigestibility, and persistence of the PEG moiety in the body (37–39). Along with these improvements, modulation of the precise length of the PAS moiety (via the number of sequence repeats in the coding gene) allows for fine-tuning of the protein hydrodynamic volume, which correlates with plasma half-life (27).

In the effort to create a functional IL-1Ra analog that escapes glomerular filtration by size exclusion, and hence increases its functional half-life, PAS–IL-1Ra protein analogs were recently developed (40). Here, we demonstrate the efficacy of the PAS600–IL-1Ra and PAS800–IL-1Ra analogs *in vitro* and *in vivo*.

Results

PAS600–IL-1Ra shows extended plasma half-life and efficacy in vivo

To investigate the half-life of PAS–IL-1Ra, 10 mg/kg PAS600–IL-1Ra (147.1 nmol/kg, see Fig. S1 for PAS–IL-1Ra molecular masses by electrospray ionization MS) or 10 mg/kg anakinra (579.5 nmol/kg) were administered subcutaneously in C57Bl/6 mice (Fig. 1). Mice were bled from the orbital plexus with heparinized capillary tubes at regular intervals. As shown in Fig. 2*A*, 24 h post-injection, the level of IL-1Ra in the blood plasma of the anakinra group was undetectable by ELISA; in contrast, a mean of 114.0 ± 34.0 ng/ml IL-1Ra (6.63 ± 1.97 pM) was detected in the PAS600–IL-1Ra group. This level was measured following the administration of 3.90 nmol of PAS600–IL-1Ra, which is 25.4% of the mole-equivalent ana-

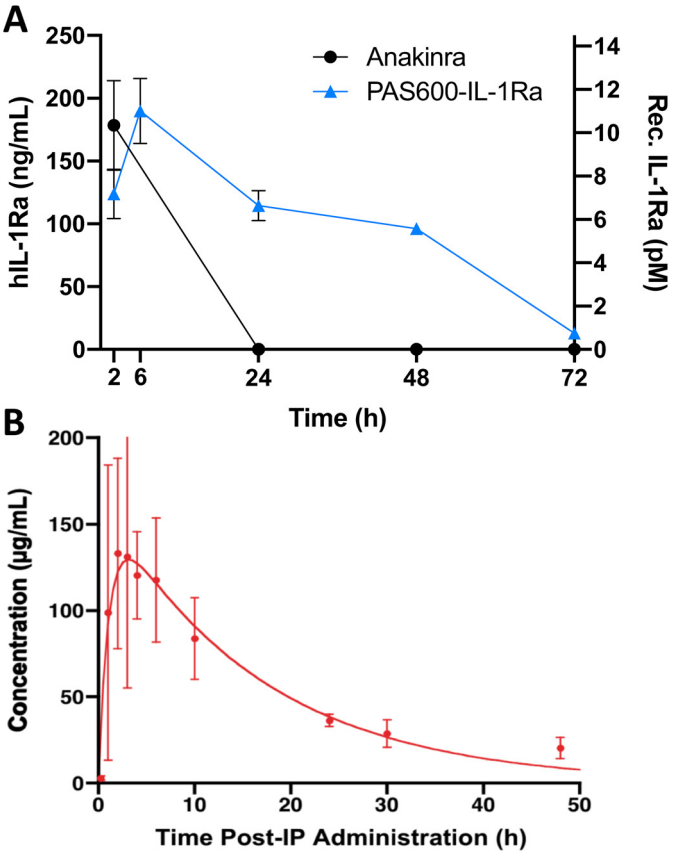

Figure 2. PAS600–IL-1Ra exhibits an extended plasma half-life. *A,* plasma levels of IL-1Ra in mice administered subcutaneously with 10 mg/kg (579.5 nmol/kg) anakinra or 10 mg/kg (147.1 nmol/kg) PAS600–IL-1Ra. $n = 3$. *B,* blood plasma concentrations of PAS600–IL-1Ra after i.p. administration in mice displayed pharmacokinetics according to the Bateman function, revealing fast biodistribution and a terminal elimination half-life $\tau_{\beta 1/2} = 11.3 \pm 2.3$ h. For comparison, a $\tau_{\beta 1/2}$ value of 2 min was reported for unmodified IL-1Ra (25). Data are presented as mean ± S.D.

kinra dose (15.4 nmol). Human IL-Ra–specific ELISA detected equimolar anakinra and PAS600–IL-1Ra at similar quantities (Fig. S2). These data reveal the extended half-life of PAS600–IL-1Ra at 3 days post-administration. In addition to the larger molecular size of PAS600–IL-1Ra, the extended half-life could in part be due to a possible "depot" effect at the subcutaneous site. For example, molecules with a large hydrodynamic size, including PEGylated proteins of different molecular weight PEGs, are prone to retention at the administration sites (41).

To investigate a possible depot effect, 15 mg/kg (220.6 nmol/kg) PAS600–IL-1Ra was instilled intraperitoneally (i.p.) in BALB/c mice, and blood plasma was collected at specific intervals (Fig. 2*B*). IL-1Ra detected in the blood plasma closely followed the Bateman function, with distinct rapid distribution and slow elimination phases (42).

To test the efficacy of the PAS600–IL-1Ra molecule, we used a well-described IL-1β–mediated mouse inflammation model where anakinra has broad anti-inflammatory effects (43). In this model, MSU crystals were instilled i.p.; after 4 h the mice were sacrificed, and the severity of peritonitis and systemic inflammation was determined. Mice were treated with 0.8 mg/kg (11.8 nmol/kg) PAS600–IL-1Ra 48 h before MSU crystal challenge. 6 h post-MSU crystal challenge, the i.p. fluid of PAS600–IL-1Ra–treated mice contained significantly less MPO (−59.0%, $p = 0.023$), a measurement of IL-1–mediated neutrophil degranulation, as compared with vehicle-treated mice (Fig. 3*B*). 48 h after i.p. instillation, PAS600–IL-1Ra was still detectable in the i.p. fluid (Fig. 3*C*), demonstrating partial retention of the molecule at the administration site.

PAS800–IL-1Ra reduces leukocyte influx and cytokines in MSU-crystal–induced peritonitis

We next investigated a larger PASylated IL-1Ra, PAS800–IL-1Ra. PAS800–IL-1Ra has an 800-residue Pro/Ala/Ser chain on its N terminus, compared with the 600-residue N-terminal chain on PAS600–IL-1Ra, comprising the same 20-mer proline, alanine, and serine sequence repeat (PAS#1) (27). These additional residues further increase the molecule's hydrodynamic volume, as discussed previously (40). We again used the MSU-crystal–induced peritonitis model. 48.3 mg/kg PAS800–IL-1Ra (579.5 nmol/kg) was administered i.p. 5 days before MSU-crystal–induced peritonitis challenge. For comparison, equimolar anakinra or PBS vehicle was administered i.p. 24 h before peritonitis. After 4 h, the mice were sacrificed. 5 days after mice had received PAS800–1Ra, a mean level of 77.20 ± 62.60 pM PAS–IL-1Ra was present in the i.p. fluid (Fig. 4*E*). In the anakinra-treated mice, the mean IL-1Ra level was considerably lower (4.43 ± 4.62 pM), demonstrating extended retention of the PAS800–IL-1Ra molecule *in vivo*.

As shown in Fig. 4*A*, there were significantly reduced numbers of lymphocytes (−26.9%, $p = 0.003$), monocytes (−37.7%, $p = 0.0003$), and granulocytes (−45.0%, $p = 0.0004$) present in the peritoneal cavity as compared with vehicle treatment. By comparison, the equimolar anakinra dose administered i.p. 24 h before MSU-crystal peritonitis challenge failed to significantly reduce lymphocytes (−4.1%, $p = 0.68$), monocytes (−8.4%, $p = 0.47$), or granulocytes (−8.3%, $p = 0.47$). PAS800–IL-1Ra–treated mice also showed reductions in IL-6 (−67.2%, $p = 0.012$), G-CSF (−76.8%, $p < 0.0001$), and MPO (−37.2%, $p = 0.052$) in the i.p. fluid (Fig. 4, *B–D*). In comparison, anakinra-treated mice showed no significant change in IL-6 (−16.7%, $p = 0.65$), G-CSF (−17.8%, $p = 0.27$), and MPO (+32.2%, $p = 0.37$).

Circulating markers of IL-1–mediated inflammation were also significantly reduced in PAS800–IL-1Ra–treated mice, including blood plasma G-CSF (−76.6%, $p < 0.0001$) and IL-6 (−57.1%, $p = 0.0003$) (Fig. 5, *A* and *B*). Anakinra-treated mice showed no significant change in these markers. IL-1Ra blood plasma levels in PAS800–IL-1Ra–treated mice averaged 27.7 ng/ml (1.6 nM) at the time of sacrifice, where blood plasma IL-1Ra levels in anakinra-treated mice were undetectable (below baseline detection in vehicle mice) (Fig. 5*C*).

To investigate whether PAS800–IL-1Ra or anakinra reduce inflammatory cytokine production from circulating white blood cells (WBC), we also cultured whole blood from these mice. To normalize for differences in WBC counts of mice, circulating blood leukocytes were used to calculate picograms of mouse IL-6 per leukocyte by group (vehicle $\bar{x} = 3.79 \times 10^6$/ml, anakinra $\bar{x} = 3.57 \times 10^6$/ml, and PAS800–IL-1Ra $\bar{x} = 3.50 \times 10^6$/ml). Total blood leukocyte counts were not significantly different between treatment groups (Fig. S3). After 24 h in culture, *ex vivo* spontaneous IL-6 secretion per million leukocytes

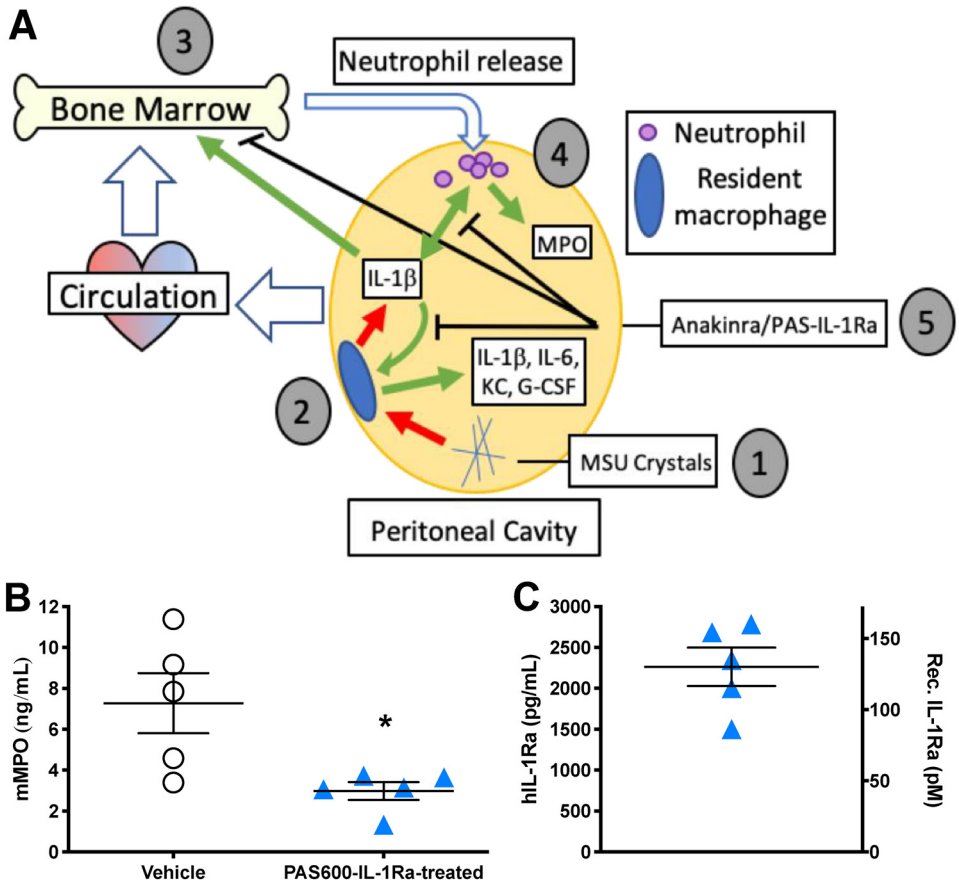

Figure 3. PAS600–IL-1Ra reduces MSU-crystal peritoneal inflammation. *A,* graphical abstract of experimental MSU-induced peritonitis. *1*) MSU crystals stimulate the release of inflammatory cytokines from *2*) resident peritoneal macrophages, including IL-1β, IL-6, KC, and G-CSF. *3*) Secreted cytokines entering the circulation stimulate neutrophil release from the bone marrow, which enters the bloodstream and reaches the peritoneal cavity. *4*) The inflammatory milieu in the peritoneal cavity stimulates further cytokine and MPO release from infiltrating neutrophils. *5*) Anakinra or PAS–IL-1Ra pretreatment inhibits IL-1 signaling in resident macrophages, the bone marrow, and infiltrating neutrophils, reducing the host inflammatory response. *B,* mean i.p. fluid MPO 6 h after MSU crystal challenge. *C,* mean i.p. fluid human IL-1Ra (in pg/ml or pM, see under "Experimental procedures") in PAS600–IL-1Ra–treated mice 6 h after MSU challenge. *B* and *C*, $n = 5$, one point represents one mouse. Data presented as mean ± S.E.; *, $p < 0.05$ (two-tailed Student's *t* test).

were significantly reduced in PAS800–IL-1Ra–treated mice (−31.9%, $p = 0.011$), but not in anakinra-treated mice (−2.1%, $p = 0.87$) (Fig. 5*G*). Circulating leukocyte populations were not significantly different between treatment groups (data not shown).

We next administered equimolar (579.5 nmol/kg) anakinra and PAS800–IL-1Ra, respectively, at the same time. We selected a 6-h pretreatment based on previous studies of anakinra in MSU-crystal–induced peritonitis. As shown in Fig. 6, anakinra pretreatment reduced levels of IL-6 (−57.7%, $p = 0.095$) and G-CSF (−35.5%, $p = 0.33$) in the i.p. fluid (Fig. 6, *A* and *B*) and IL-6 (−20.5%, $p = 0.63$) and G-CSF (−50.3%, $p = 0.27$) in the blood plasma (Fig. 6, *D* and *E*), although not significantly, due to a pronounced outlier. PAS800–IL-1Ra significantly reduced levels of IL-6 (−96.2%, $p = 0.0005$) and G-CSF (−70.6%, $p = 0.0027$) in the i.p. fluid (Fig. 6, *A* and *B*) and IL-6 (−70.0%, $p = 0.001$) and G-CSF (−82.8%, $p < 0.0001$) in the blood plasma (Fig. 6, *D* and *E*). Mice in the PAS800–IL-1Ra group also showed reduced blood lysate G-CSF (−85.7%, $p = 0.0051$, Fig. 6*G*) and KC (−58.1%, $p = 0.069$, Fig. 6*H*), where anakinra-treated mice experienced lesser reductions in G-CSF (−35.3%, $p = 0.30$) and no reduction in KC (+6.8%, $p = 0.87$). We detected less spontaneous IL-6 in whole-blood culture supernatants from PAS800–IL-1Ra–treated mice (−58.0%, $p = 0.002$, Fig. 6*I*), where anakinra-treated mice showed a smaller reduction (−29.7%, $p = 0.21$). There were no significant differences in circulating leukocyte populations (data not shown). At sacrifice, PAS800–IL-1Ra–treated mice had more than 25-fold more detectable IL-1Ra in the i.p. fluid as compared with anakinra-treated mice (7.43 nM *versus* 0.29 nM), and more than 176-fold more detectable IL-1Ra in the blood plasma (69.89 nM *versus* 0.40 nM). Thus, in a more acute model, PAS800–IL-1Ra still results in a large differential of local and circulating IL-1Ra as compared with anakinra.

Comparison of anakinra, PAS600–IL-1Ra., and PAS800–IL-1Ra for reduction of IL-1-dependent signaling in vitro

A549 cells are immortalized bronchial epithelial adenocarcinoma cells that respond to IL-1, producing IL-6 and IL-8 (44). A549 cells were treated with or without anakinra, PAS600–IL-1Ra, or PAS800–IL-1Ra 1 h before the addition of IL-1α. After 24 h of culture, significant dose-dependent reductions in secretion of IL-6 (Fig. 7*A*) and IL-8 (Fig. 7*B*) were observed for PAS600–IL-1Ra (−85.0% IL-6, $p < 0.0001$; −66.1% IL-8, $p = 0.0023$), PAS800–IL-1Ra (−83.0% IL-6, $p < 0.0001$; −66.3% IL-8, $p = 0.0025$), and anakinra (−97.5% IL-6, $p < 0.0001$;

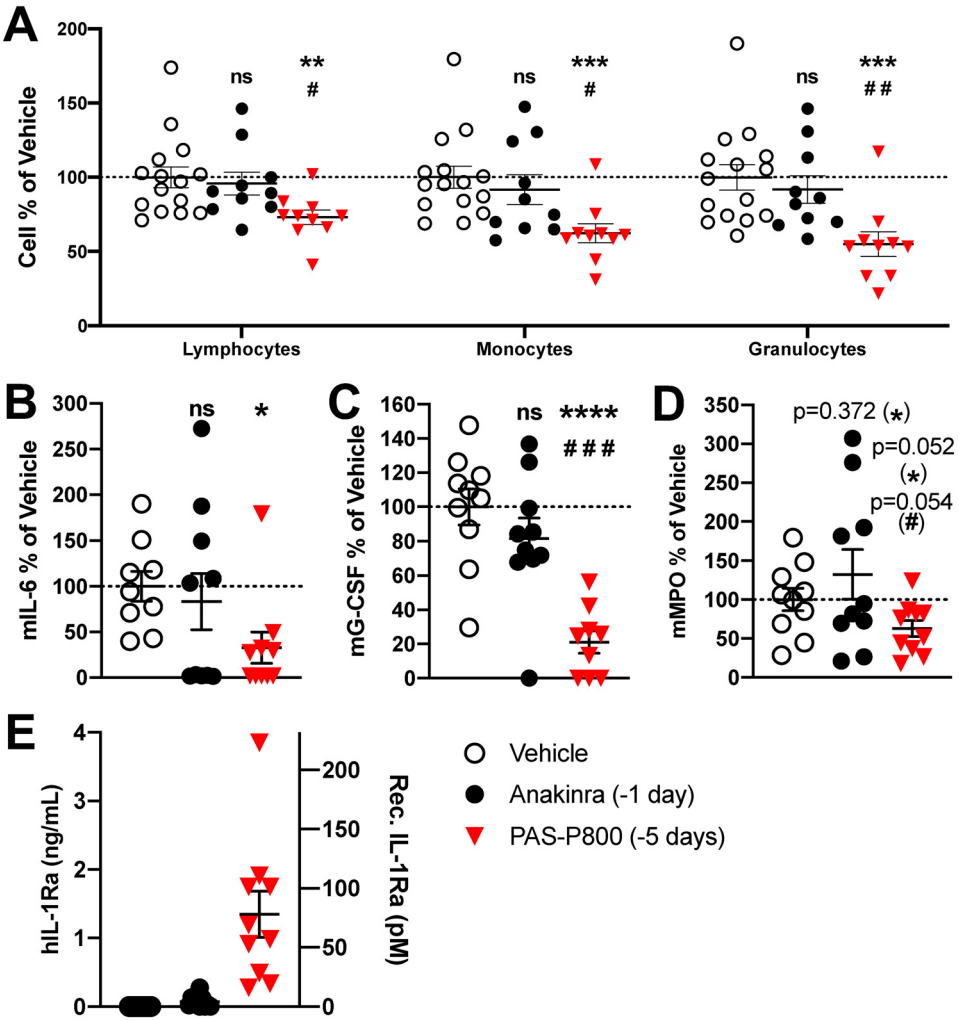

Figure 4. Comparison of 5-day PAS800–IL-1Ra and 1-day anakinra pretreatment efficacy in MSU-crystal–induced peritonitis. *A,* peritoneal leukocyte populations were assessed in i.p. fluid by automated cell counter (vehicle ranges: lymphocytes, 0.83–2.24 × 10^6/ml; monocytes, 0.44–0.84 × 10^6/ml; granulocytes, 1.08–2.02 × 10^6/ml). Mouse IL-6 (*B*) (vehicle range 138–8620 pg/ml), mouse G-CSF (*C*) (vehicle range 111–559 pg/ml), mouse MPO (*D*) (vehicle range 2.42–39.80 ng/ml), and human IL-1Ra (*E*) in the i.p. fluid 4 h after i.p. instillation of MSU (120 mg/kg) are shown. *B–D,* data are expressed as percent change from the vehicle group mean of each experiment, with the vehicle group mean set at 100%. Then, cytokine levels or cell counts from each mouse were expressed as percentage of the vehicle mean. Experiments 1 (5 mice) and 2 (5 mice) were then combined; one point represents one mouse. Data presented as mean ± S.E.; *ns,* not significant; *, $p < 0.05$; **, $p < 0.01$; ***, $p < 0.001$; and ****, $p < 0.0001$ (vehicle/PAS800–IL-1Ra comparison); #, $p < 0.05$; ##, $p < 0.01$; and ###, $p < 0.001$ (anakinra/PAS800–IL-1Ra comparison) (two-tailed Student's *t* test).

−84.0% IL-8, $p < 0.0001$). Reductions of IL-6 and IL-8 between PAS600–IL-1Ra and PAS800–IL-1Ra were not significantly different at any equivalent dose. Pretreatments at equimolar concentrations (579.5 nM) showed similar reductions of IL-6 and IL-8 secretion, suggesting comparable IL-1 signal inhibition.

The effect of PAS600–IL-1Ra and PAS800–IL-1Ra was also tested in PBMC. We used stimulation with heat-killed *Candida albicans* to induce IL-22, as IL-22 is immunosuppressive in murine models of human cancer and is inhibited by anakinra (45). Therefore, we used an equimolar concentration of anakinra for comparison. After 5 days, the level of IL-22 in cell culture supernatants was significantly reduced by PAS600–IL-1Ra (−56.0%, $p = 0.0034$ at 579.5 nM) and PAS800–IL-1Ra (−54.0%, $p = 0.0003$ at 579.5 nM). Reductions of IL-22 between PAS600–IL-1Ra and PAS800–IL-1Ra were not significantly different at any equivalent dose (Fig. 7*C*). Similarly, anakinra significantly reduced IL-22 secretion at equimolar doses to PAS600–IL-1Ra and PAS800–IL-1Ra (−84.7%, $p < 0.0001$ at 579.5 nM).

Because equimolar concentrations of anakinra were more effective in suppressing IL-6, IL-8, and IL-22 *in vitro*, we compared the binding activities of PAS600–IL-1Ra, PAS800–IL-1Ra, and anakinra to the immobilized extracellular domains of the human IL-1R1. Real-time affinity measurements by SPR spectroscopy are depicted in Fig. 8. Both PAS–IL-1Ra versions retained high receptor-binding activity. In line with the cell culture experiments, fusion of IL-1Ra with a PAS#1(800) sequence (creating PAS800–IL-1Ra) led to a moderate 6-fold decrease in IL-1R1 affinity, which was mainly due to a slower association rate (k_{on} of 2.23 × 10^5 M^{-1} s^{-1}, as compared with 9.82 × 10^5 M^{-1} s^{-1} for anakinra, see Table 1).

Discussion

Because PASylating proteins for clinical use leads to greater circulating half-lives, these proteins show extended efficacy fol-

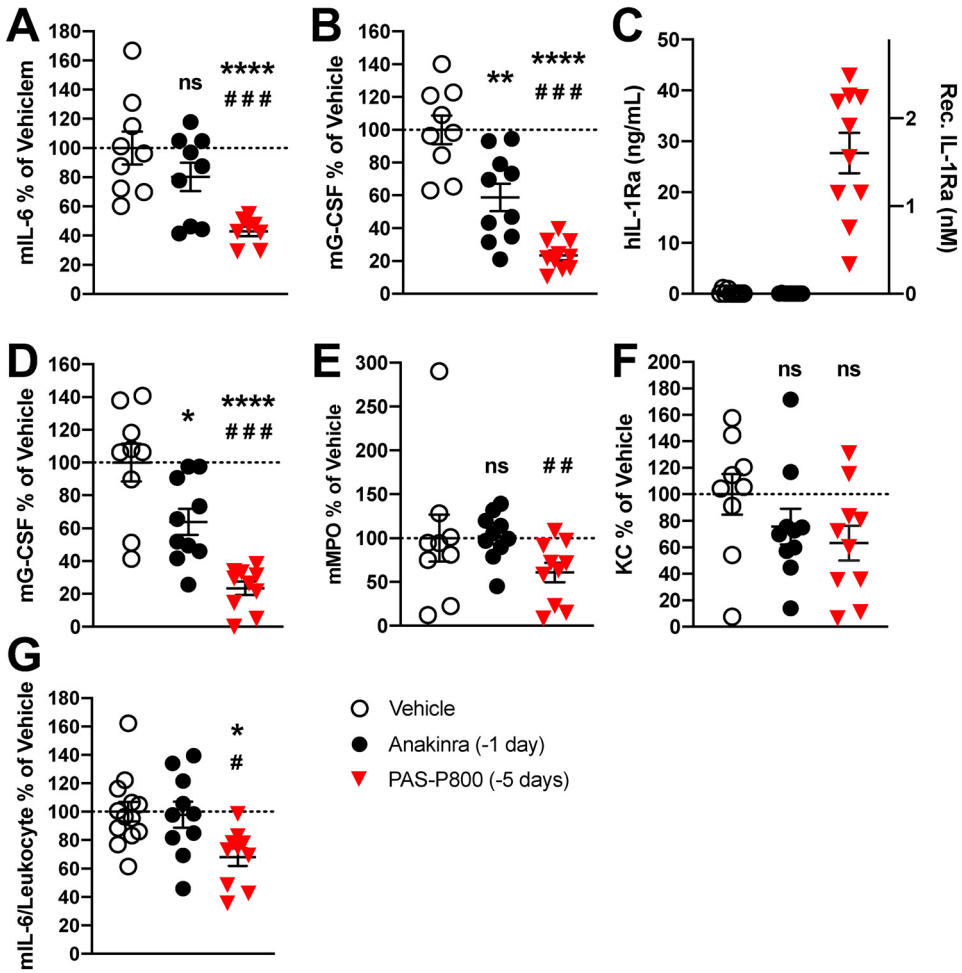

Figure 5. Comparison of 5-day PAS800–IL-1Ra and 1-day anakinra pretreatment in systemic inflammation in MSU-peritonitis. *A–C,* plasma levels of mouse IL-6 (*A*), vehicle range 149–2920 pg/ml, mouse G-CSF (*B*), vehicle range 3.71–15.30 ng/ml, and human IL-1Ra (*C*). *D–F,* remaining blood pellet was lysed in 0.5% Triton X-100 following centrifugation and assayed for mouse G-CSF (*D*), mouse MPO (*E*) (2.92–333.47 ng/ml), and KC (*F*) (551–11578 pg/ml). Whole blood, diluted 1 part in 5, was cultured for 24 h. Supernatants were assayed for mouse IL-6 (*G*). Absolute IL-6 (vehicle range 17.5–37.0 pg/ml) was normalized per million of circulating leukocytes (see "Results"). Data are expressed as percent change from the vehicle group mean of each experiment, with the vehicle group mean set at 100%. Experiments 1 (5 mice) and 2 (5 mice) were then combined, and one point represents one mouse. Data are presented as mean ± S.E.; *ns*, not significant; *, $p < 0.05$; **, $p < 0.01$; ***, $p < 0.001$; and ****, $p < 0.0001$ (control/PAS800–IL-1Ra comparison); #, $p < 0.05$; ##, $p < 0.01$; and ###, $p < 0.001$ (anakinra/PAS800–IL-1Ra comparison) (two-tailed Student's *t* test).

lowing administration. Anakinra is the recombinant form of naturally-occurring IL-1Ra used to treat a broad spectrum of inflammatory diseases (14); however, anakinra requires daily administration. Hence, PASylation® of IL-1Ra would reduce the need for daily injections. Patient adherence to medication is a major challenge in treating disease effectively (46), and in the case of anakinra, discomfort following subcutaneous injection can result in missed doses and decreased therapeutic effect. Furthermore, gout patients show low treatment adherence and persistence in their 1st year of therapy (36.8%), in part due to daily injections (47). Reducing the frequency of injections in gout while retaining therapeutic effect could greatly increase patient quality of life and adherence to treatment. A longer-lasting IL-1Ra would require less frequent administration, addressing these concerns. Moreover, PASylated IL-1Ra would result in a longer-lasting steady-state drug level in circulation and enhanced pharmacological effect due to saturation levels and prolonged IL-1R1 occupancy. Thus, the major goals of this investigation were to investigate extension of IL-1Ra half-life via PASylation® and the resulting IL-1 blockade activity and efficacy.

As with PASylated molecules previously investigated (35), PAS600–IL-1Ra demonstrates increased plasma retention. In this study, we evaluated PAS600–IL-1Ra pharmacokinetics in mice. As shown in Fig. 2, a single administration of 10 mg/kg (147.1 nmol/kg) PAS600–IL-1Ra administered subcutaneously in mice was detectable in plasma after 3 days. On a mass basis, PAS600–IL-1Ra outlasts anakinra in the circulation. Similarly, PAS600–IL-1Ra instilled i.p. showed extended pharmacokinetics. Both subcutaneous and i.p. administration led to peak plasma PAS–IL-1Ra levels 6 h later, indicating rapid absorption into the circulation regardless of the administration site.

With the extended half-life of PAS–IL-1Ra, we examined its efficacy *in vivo*. We chose a model where IL-1 blockade has established efficacy: MSU-crystal–induced inflammation (14). In gouty arthritis attacks, MSU crystals stimulate synovial macrophages to initiate local inflammation by IL-1β secretion, which induces chemokines such as IL-8 that attract monocytes

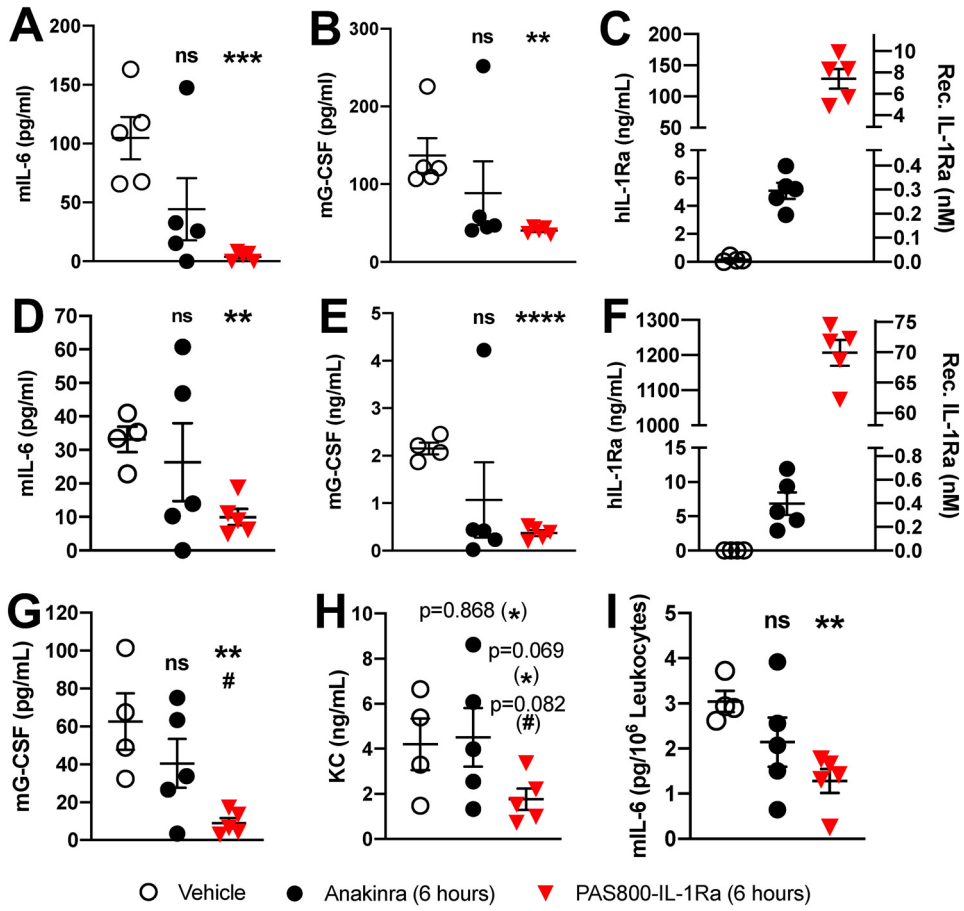

Figure 6. 6-h pretreatment with PAS800–IL-1Ra and anakinra reduce inflammation in MSU-crystal–induced peritonitis. *A–C,* i.p. fluid concentrations of mouse IL-6 (*A*), mouse G-CSF (*B*), and human IL-1Ra (*C*) 4 h after i.p. MSU crystal instillation, as in Fig. 5. *D–F,* plasma concentrations of mouse IL-6 (*D*), mouse G-CSF (*E*), and human IL-1Ra (*F*) from the same experiment. *G* and *H,* remaining blood pellet was lysed with 0.5% Triton X-100, as in Fig. 5, and assayed for mouse G-CSF (*G*) and KC (*H*). Whole blood, diluted 1 part in 5, was cultured for 24 h and then the supernatant was assayed for mouse IL-6 (*I*), as in Fig. 5. Data are presented as mean ± S.E.; *ns,* not significant;*, $p < 0.05$; **, $p < 0.01$; ***, $p < 0.001$; and ****, $p < 0.0001$ (Control/PAS800–IL-1Ra comparison); #, $p < 0.05$ (Anakinra/PAS800–IL-1Ra comparison) (two-tailed Student's *t* test).

and neutrophils (48). In mice, MSU-crystal–induced peritonitis provides a gout-like model (48).

PAS600–IL-1Ra was first investigated in MSU-crystal peritonitis. Administering 0.8 mg/kg (11.8 nmol/kg) PAS600–IL-1Ra 2 days (48 h) before MSU crystal challenge significantly reduced MPO in the peritoneal exudate fluid. MPO serves as a marker of neutrophil influx and activation, which is IL-1–dependent. This amount of PAS–IL-1Ra (0.8 mg/kg) represents 2% of the 10 mg/kg anakinra dose used in later investigations by molarity. Nevertheless, PAS–IL-1Ra provided anti-inflammatory activity comparable with a higher dose of anakinra given closer to peritonitis onset.

PASylation® allows increasing half-life extension as the PAS moiety is elongated. Thus, we investigated the potency of PAS800–IL-1Ra as a longer PAS–IL-1Ra conjugate. PAS800–IL-1Ra administered 5 days (120 h) before MSU crystal challenge markedly reduced leukocyte infiltration and IL-1–mediated inflammation (Figs. 4 and 5). The effectiveness of PAS800–IL-1Ra in the same model as PAS600–IL-1Ra supports a general conservation of inhibitory potency among PAS–IL-1Ra analogs with different molecular weights. Furthermore, the longer effective half-life of PAS800–IL-1Ra as compared with PAS600–IL-1Ra supports the reported relationship between PAS moiety length and half-life (40).

But how does dosing every 5 days in mice relate to humans? In general, mice have reduced half-lives of small molecules and proteins compared with larger mammals (35). This implies a potentially longer effective half-life for PAS800–IL-1Ra in humans at equivalent doses. Notably, anakinra dosing 24 h before peritoneal MSU crystal challenge in mice showed little efficacy in reducing inflammation or leukocyte infiltration (Figs. 4 and 5). Given the efficacy of daily anakinra in humans, weekly PAS800–IL-1Ra dosing may have similar therapeutic efficacy (42).

Comparison of PAS–IL-1Ra at extended dosing schedules does not address the question of efficacy in an acute model. Anakinra is known for its rapid anti-inflammatory effects in multiple conditions, including gout flares (14). Whether rapid efficacy of is also observed for PAS–IL-1Ra is an issue. In a head–to–head comparison of equimolar anakinra and PAS800–IL-1Ra, PAS800–IL-1Ra equaled or exceeded the anti-inflammatory effects of anakinra when both were given 6 h before MSU challenge (Fig. 6). Of note, the plasma levels of IL-1Ra in PAS800–IL-1Ra- and anakinra-treated mice differed

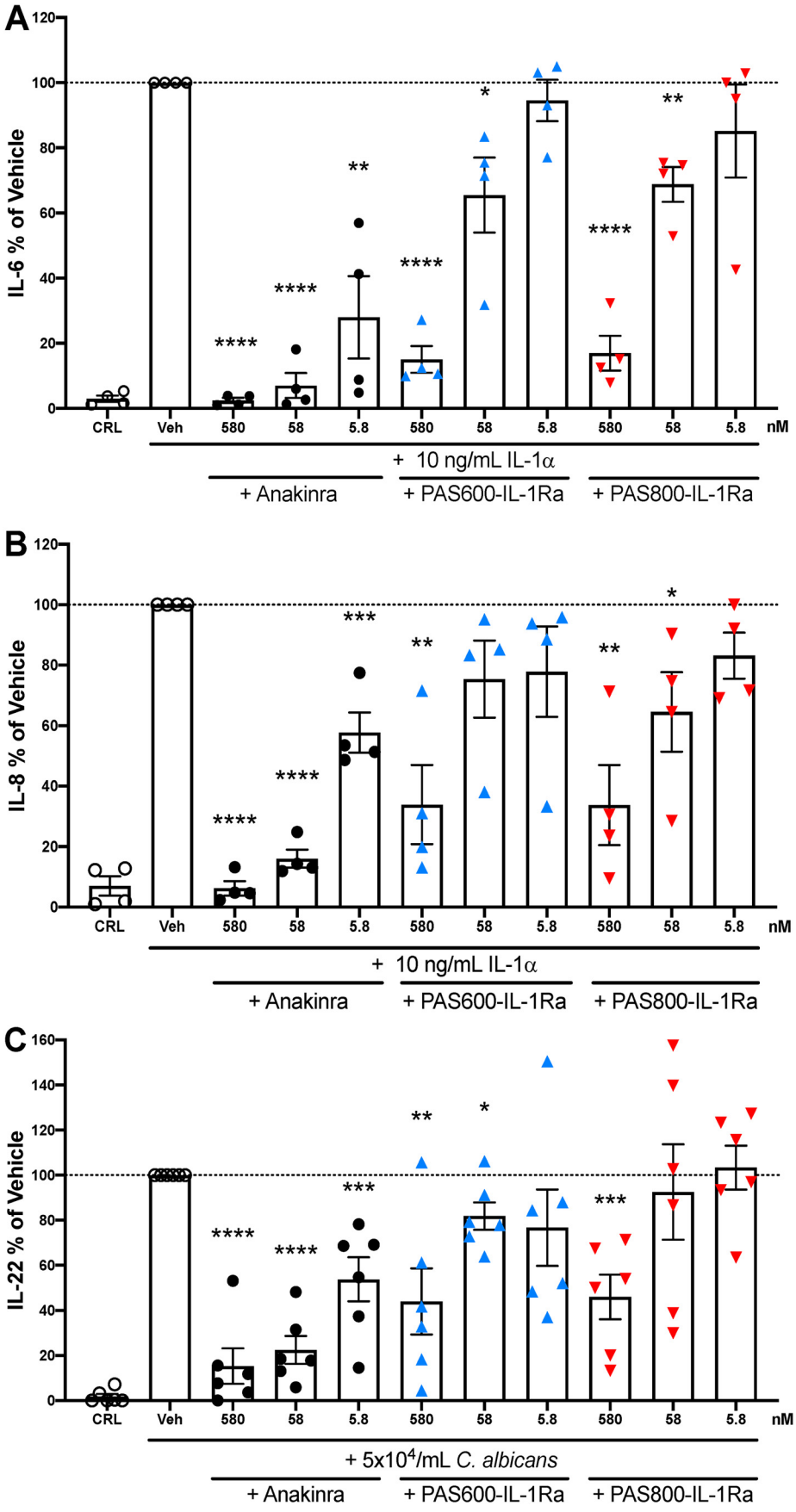
A
IL-6 % of Vehicle
120
100
80
60
40
20
0
CRL
Veh
580
58
5.8
580
58
5.8
580
58
5.8
nM
+ 10 ng/mL IL-1α
+ Anakinra
+ PAS600-IL-1Ra
+ PAS800-IL-1Ra
B
IL-8 % of Vehicle
120
100
80
60
40
20
0
CRL
Veh
580
58
5.8
580
58
5.8
580
58
5.8
nM
+ 10 ng/mL IL-1α
+ Anakinra
+ PAS600-IL-1Ra
+ PAS800-IL-1Ra
C
IL-22 % of Vehicle
160
140
120
100
80
60
40
20
0
CRL
Veh
580
58
5.8
580
58
5.8
580
58
5.8
nM
+ 5x10⁴/mL C. albicans
+ Anakinra
+ PAS600-IL-1Ra
+ PAS800-IL-1Ra

by 176-fold between the administration and the end of the experiment (Fig. 6, *C* and *F*). The rapid decline of circulating anakinra concentrations as compared with PAS800–IL-1Ra likely explains the difference of efficacy, and it highlights a likely clinical outcome of PAS800–IL-1Ra use. Because PAS–IL-1Ra has reduced IL-1 receptor blockade activity as compared with anakinra, the high level of circulating PASylated IL-1Ra compensates for the lower affinity and renders a more effective IL-1 receptor blockade compared with anakinra. Comparing inflammatory cytokine markers between experiments further illustrates the immediate and long-term improvements of PAS–IL-1Ra efficacy over anakinra (Fig. S4).

Will PAS–IL-1Ra therapy show a qualitative improvement over current anakinra therapy? The data suggest that PAS–IL-1Ra improves therapeutic response as compared with anakinra in short- and long-term dosage. For example, direct cytokine and leukocyte measurements demonstrate PAS800–IL-1Ra outperforms anakinra in IL-1 receptor blockade, even over several days (Figs. 4 and 5). Furthermore, the maintenance of high circulating IL-1Ra levels could prevent concentration "troughs" of IL-1Ra between doses. Given the rapid clearance of anakinra, patients are treated with daily administration. By slowing the clearance of IL-1Ra in circulation and reducing the number of weekly injections required for IL-1 receptor blockade, PAS–IL-1Ra could prevent concentration troughs. Without rapid drops of IL-1Ra levels characteristic of daily anakinra, intermittent IL-1 signaling spikes would occur less frequently. In a recent analysis, recurrent gouty arthritis attacks while on medication was a major factor for treatment noncompliance (49). Some patients, sensing the drug was not effective, stopped treatment. PAS–IL-1Ra will likely be used in chronic IL-1–mediated conditions such as RA and osteoarthritis (50), along with atherosclerosis (51), type 2 diabetes (52, 53), and heart failure (54, 55), each of which can occur in patients with recurrent attacks of gout and is effectively treated in humans by reducing IL-1 signaling (50).

To support an IL-1–specific inhibitory mechanism by PAS–IL-1Ra, the IL-1–responsive A549 cell line was employed to test IL-1 blockade. IL-1α stimulated IL-6 (Fig. 7*A*) and IL-8 (Fig. 7*B*) release, which was attenuated in a dose-dependent manner by anakinra, and was similarly reduced by PAS600–IL-1Ra and PAS800–IL-1Ra at equivalent molarities. Similar dose-dependent reductions in IL-22 were observed for *C. albicans*–stimulated human PBMC (Fig. 7*C*). Reductions in IL-1–dependent cytokine release in cell assays support the direct IL-1 blockade capabilities of PAS–IL-1Ra.

We also examined the inhibitory activity of PAS–IL-1Ra on the production of IL-22. IL-22, a member of the IL-10 family, increases proliferation of malignant cells, tumor progression, and immunosuppression (45). Thus, IL-22 has become a key target for immune checkpoint inhibition in cancers of epithelial origin, including lung, liver, colon, breast, and gastric cancers (45). In humans, breast cancer cells induce IL-1β from myeloid and lymphoid cells, which stimulates IL-22 release from diverse lymphoid cells. Disrupting this IL-1 signal with IL-1Ra reduced IL-22 levels and IL-22–producing cell numbers in two breast cancer models, and coincided with slowed tumor growth (45). From this, IL-1 blockade shows promise as a checkpoint inhibition strategy in cancer. As we have demonstrated, PAS–IL-1Ra not only retains IL-1 blockade activity but also inhibits downstream stimulation of IL-22 in PBMC. Because IL-22 is exclusively produced by immune cells such as those in PBMC, systemic IL-1 blockade through IL-1Ra may be capable of broad IL-22 inhibition. Furthermore, blocking IL-22 upstream may be preferable to direct IL-22 depletion therapy, which may disrupt intestinal inflammatory balance, hinder clearance of intestinal infections, and affect intestinal microbiota populations (56). Accordingly, PAS–IL-1Ra could be administered as a long-lasting immune checkpoint inhibitor of IL-22–mediated cancer growth and progression. Greatly increased retention of PAS–IL-1Ra may even augment the anticancer efficacy of IL-1 receptor blockade (1, 57).

Investigation of PAS–IL-1Ra in cell assays showed moderate reductions in IL-1 inhibition potency as compared with anakinra at equimolar concentrations (Fig. 7). To investigate these differences in potency *in vitro*, and to investigate direct IL-1R1 binding by PAS–IL-1Ra, SPR analysis was used (Fig. 8). The data reveal direct binding of PAS–IL-1Ra to IL-1R1, similar to anakinra. The higher receptor K_D seen for PAS–IL-1Ra may be the source of reduced *in vitro* activity. Reduction in target affinity is also well-known for other polymers, including PEG, which may be caused by a slower-diffusion rate due to the enlarged molecular dimensions of the conjugate (58). Nevertheless, this effect is likely overcompensated *in vivo* due to the much-prolonged plasma half-life. Understandably, this cannot be simulated in a cell culture assay. According to the Law of Mass Action, receptor binding *in vivo* is governed both by drug affinity and its circulating concentration. Because PASylation® dramatically extends the circulating drug life span, efficient receptor blocking is strongly favored *in vivo*, as demonstrated with the mouse data presented here for PAS–IL-1Ra.

For PAS–IL-1Ra to become an effective treatment, it must demonstrate safety. Concerns of vacuolization and immunogenicity in similar PEGylated proteins have been raised (37–39). But if PAS–IL-1Ra shares properties common to other PASylated proteins, including extended plasma retention, conserved function, and retarded migration in SDS-PAGE (Fig. S5), it likely also shares their safety profile. Data from PASylated protein studies in nonhuman primates are particularly relevant, because no adverse effects were observed following chronic dosing (36, 59). Recently, a PASylated i-body conjugated with a 600-residue PAS polypeptide similar to that of PAS600–IL-1Ra showed no adverse effects in cynomolgus monkeys at doses up

Figure 7. Comparison between anakinra and PASylated IL-1Ra in A549 cells and human PBMC. *A* and *B*, A549 cells were stimulated for 24 h with recombinant human IL-1α. Experimental $n = 4$, vehicle IL-6 range 2.03–12.62 ng/ml (*A*) and vehicle IL-8 range 13.2–36.3 ng/ml (*B*). *C*, PBMC from six healthy donors, stimulated 5 days with heat-killed *C. albicans*. Vehicle IL-22 range 64.6–6290 pg/ml. *A–C*, equimolar anakinra, PAS600–IL-1Ra and PAS800–IL-1Ra treatments of 5.8–580 nM are indicated *below bar graphs*. These values were calculated from MS values (Fig. S2). Data are expressed as % change from the vehicle group, with the mean of the vehicle group triplicate set at 100%. One point represents one averaged triplicate (one experimental group). Data are presented as mean ± S.E.; *, $p < 0.05$; **, $p < 0.01$; ***, $p < 0.001$; and ****, $p < 0.0001$ (two-tailed Student's *t* test).

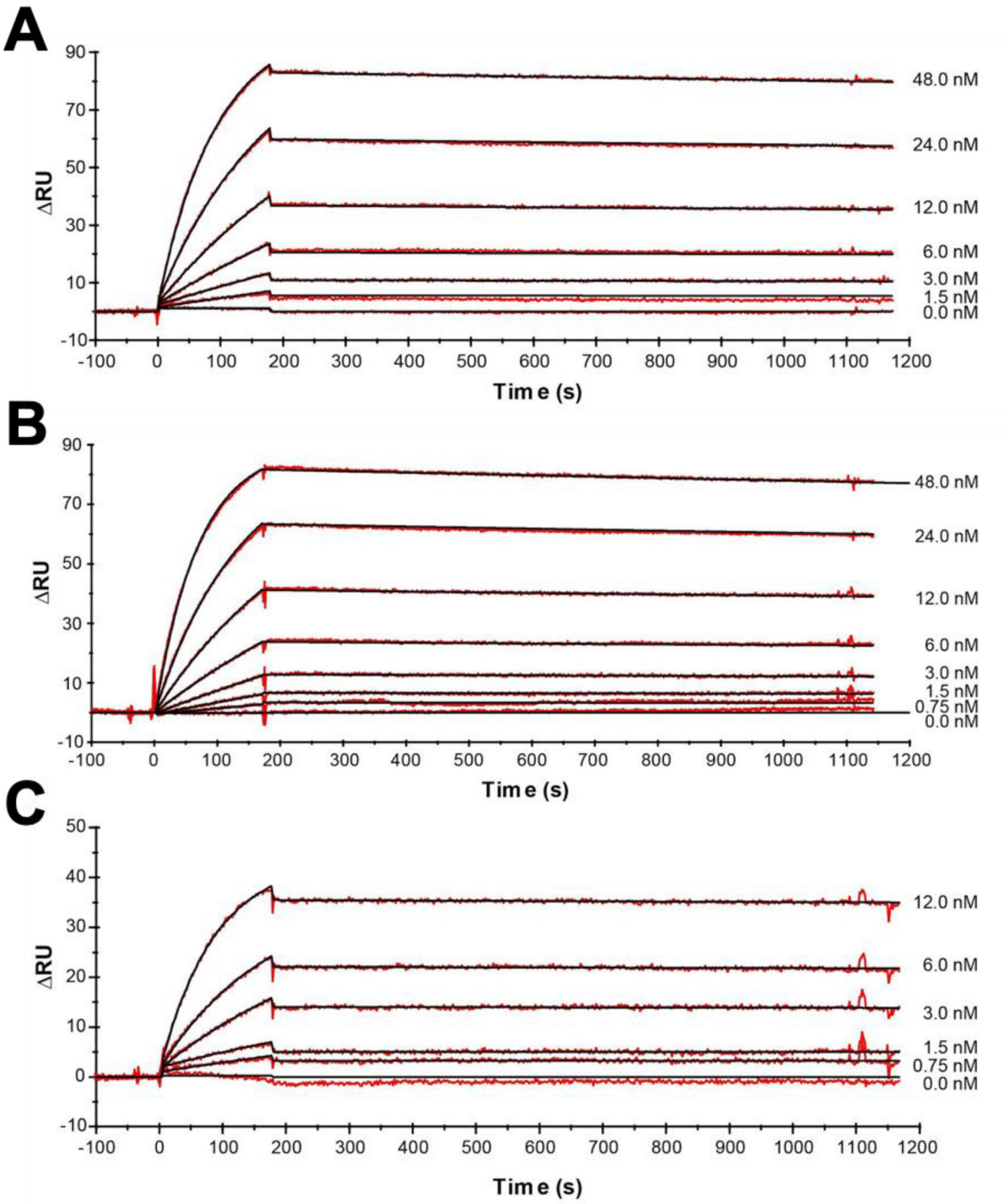

Figure 8. *In vitro* binding of PASylated IL-1Ra and anakinra. Real-time kinetic SPR analysis on a BIAcore 2000 instrument of PAS800–IL-1Ra (*A*), PAS600–IL-1Ra (*B*), and anakinra *versus* IL-1R1 (as Fc chimera) (*C*) immobilized on a CM3 sensorchip (ΔRU = 180). The signals for various ligand concentrations are depicted as *red lines* with curve fits according to a 1:1 Langmuir model shown in *black*. The resulting kinetic and affinity parameters are listed in Table 1.

to 100 mg/kg, along with the characteristic extended plasma retention and receptor-binding activity (60).

Immune responses to PAS–IL-1Ra in humans remain to be investigated. On the Food and Drug Administration–approved label for Kineret®, the manufacturer reports that 28% of RA patients tested positively for anti-anakinra antibodies after 6 months of treatment using a highly-sensitive anakinra-binding biosensor assay. Of the 1274 subjects with available data, <1%

Table 1
Kinetic parameters measured by SPR

Protein sample	k_{on} (10^5 M^{-1} s^{-1})	k_{off} (10^{-5} s^{-1})	K_D
			pM
PAS800-IL-1Ra	2.23	2.63	118
PAS600-IL-1Ra	3.02	4.29	142
Anakinra	9.82	1.82	18.5

(9 subjects) were seropositive for antibodies capable of neutralizing the biologic effects of anakinra in a cell-based bioassay. Recent long-term follow-up studies indicate that the incidence of anti-anakinra–neutralizing antibodies is extremely low (61–63). Although these values provide assurance about the relative nonimmunogenicity of recombinant IL-1Ra in patients with chronic inflammatory and autoimmune diseases, the predictability of immunogenicity of PAS–IL-1Ra in immunosuppressed patients is of considerable interest (62). The presence of anti-PAS–IL-1Ra–neutralizing antibodies will be closely monitored in clinical trials (64–66).

In summary, after applying PASylation® technology to naturally-occurring IL-1Ra, PAS600–IL-1Ra and PAS800–IL-1Ra were examined for pharmacokinetics as well as efficacy. The addition of the extended PAS moiety greatly extended the half-life of IL-1Ra without significantly reducing IL-1 receptor 1 blockade capabilities. This allowed equimolar PAS–IL-1Ra to outperform anakinra in inflammatory MSU-crystal peritonitis in mice even when administered 5 days prior to challenge. As off-label use of anakinra expands, and IL-1 signaling is implicated in several inflammatory diseases, including cancer, PAS–IL-1Ra may constitute a new treatment option.

Experimental procedures

Mice

Male C57Bl/6 mice were purchased from The Jackson Laboratory (Bar Harbor, ME) and housed in the University of Colorado Anschutz Campus vivarium. Animal groups were age-matched by birth date, and all mice were 6–8 weeks of age. Mouse protocols were approved by the Institutional Animal Care and Use Committee of the University of Colorado at Denver.

Reagents

Anakinra was the kind gift of Amgen (Thousand Oaks, CA). PASylated recombinant human IL-1Ra (*e.g.* P600–IL-1Ra) was prepared as described previously (40). For this study, a structural gene for PAS800–IL-1Ra was constructed using a longer nonrepetitive reading frame with improved genetic stability (35) and without the addition of an affinity tag. The fusion protein was produced in the cytoplasm of *Escherichia coli* Origami™ B strain (Merck Millipore, Darmstadt, Germany) in a correctly-folded state and purified in several chromatographic steps, followed by endotoxin depletion (see supporting Experimental methods). The homogeneity of PAS600-IL-1Ra and PAS800-IL-1Ra preparations, including absence of aggregates, was assessed by analytical SEC (Fig. S6). Recombinant human IL-1α was purchased from R&D Systems (Minneapolis, MN). A clinical isolate of *C. albicans* was grown in Saboraud's broth overnight, washed three times with sterile saline, counted in a hemocytometer, and boiled for 30 min. RPMI 1640 + L-glutamine, F-12K media, and heat-inactivated fetal calf serum (FCS) were purchased from Thermo Fisher Scientific (Hampton, NH). Penicillin/streptomycin, 0.25% trypsin solution (2.21 mM EDTA), and MSU crystals were purchased from Sigma.

Specific ELISA

Cytokine and MPO concentrations were analyzed via ELISA kits (DuoSet®, R&D Systems, Minneapolis, MN) as per the manufacturer's instructions. Anakinra and PAS–IL-1Ra concentrations were measured by human IL-1Ra ELISA and found to give similar detections for each molecule as compared with control IL-1Ra (Fig. S1).

For all graphs of human IL-1Ra, the left *y* axis denotes ELISA-detected human IL-1Ra (using the provided IL-1Ra standard), and the right *y* axis denotes equivalent moles of IL-1Ra (anakinra, PAS600–IL-1Ra, and PAS800–IL-1Ra have different molar weights, see Fig. S2). Molarity for all ELISA-detected IL-1Ra was calculated using the molecular mass of anakinra (17.3 kDa).

Subcutaneous PAS600–IL-1Ra dosing for subcutaneous pharmacokinetics

10 mg/kg (147.1 nmol/kg) PAS600–IL-1Ra or 10 mg/kg (579.5 nmol/kg) anakinra was injected subcutaneously in 200 μl of sterile saline in mice, and then blood was collected at 2 and 6 h (PAS600–IL-1Ra only), then 24 and 48 h, and again after 72 h. Blood was drawn in heparinized 20-μl capillary tubes (Sarstedt AG & Co., Nümbrecht, Germany) from the orbital plexus after anesthetization by isoflurane inhalation (Piramel Critical Care, Bethlehem, PA). Heparinized blood was centrifuged 10 min at 1344 × *g* at 23 °C (Heraeus Biofuge 13, Marshal Scientific, Hampton, NH), and plasma was aspirated and frozen at −20 °C for specific ELISA.

PAS600–IL-1Ra dosing for intraperitoneal pharmacokinetics

PK studies in BALB/c mice (i.p. application of 15 mg/kg body weight) were performed according to a published procedure (27). Plasma was collected from blood by centrifugation for 10 min at 1344 × *g* at 23 °C and aspiration, then plasma was flash-frozen in liquid nitrogen, and stored at −20 °C. IL-1Ra content at different time points was measured by ELISA.

MSU-crystal–induced experimental peritonitis using PAS600–IL-1Ra

Two groups of five mice were randomly assigned as control or for PAS600–IL-1Ra treatment. 48 h (2 days) before MSU stimulation, mice received i.p. 0.8 mg/kg (11.8 nmol/kg) PAS600–IL-1Ra in 200 μl of sterile saline or with 200 μl of sterile saline alone. Then mice were instilled i.p. with 3 mg of MSU crystals and sacrificed after 6 h. 10 ml of ice-cold sterile saline was rapidly infused i.p., and the fluid was collected, centrifuged for 4 min at 244 × *g* at 4 °C (5810 R centrifuge, Eppendorf, Hamburg, Germany), aspirated, and frozen at −20 °C for MPO and cytokine ELISAs.

MSU-crystal–induced experimental peritonitis using PAS800–IL-1Ra

For the first experiment, groups of five mice were randomly assigned to control, anakinra treatment, and PAS800–IL-1Ra treatment groups. 120 h (5 days) before MSU crystal instillation, mice were treated i.p. with 48.3 mg/kg (579.5 nmol/kg) PAS800–IL-1Ra in 200 μl of sterile saline (PAS800–IL-1Ra treatment group), or sterile saline alone (control group). 24 h before MSU stimulation, the anakinra treatment group mice were treated i.p. with 10 mg/kg (579.5 nmol/kg) anakinra in sterile saline. Then, all groups were instilled i.p. with 3 mg/kg MSU crystals in 200 μl of sterile saline. All mice were sacrificed 4 h after MSU administration. Blood was collected from the orbital plexus in EDTA. A portion of the whole blood was removed for culture, and then the remaining blood was centrifuged 10 min at 1344 $\times$ *g* at 23 °C. Plasma was aspirated and frozen at −20 °C for ELISA, and the remaining blood pellet was lysed with 0.5% Triton X-100 (Sigma) and frozen at −20 °C for ELISA. The peritoneal cavity was lavaged with 10 ml of ice-cold PBS and collected by puncture, and then the fluid was centrifuged for 4 min at 244 $\times$ *g* at 4 °C. The supernatant was aspirated and frozen at −20 °C for ELISA, and the pellet was resuspended in 500 μl of PBS for hematology analysis on the Heska veterinary hematology analyzer. To express the data, the mean of the vehicle group cell counts or proteins was set at 100%. Then, all points in that experiment were expressed as percent of the vehicle mean. Experiments ($n = 2$) were then combined.

For the second experiment, groups of five mice were randomly assigned to control, anakinra treatment, and PAS800–IL-1Ra treatment groups. 6 h before MSU crystal instillation, mice were treated i.p. with 48.3 mg/kg (579.5 nmol/kg) PAS800–IL-1Ra in 200 μl of sterile saline (PAS800–IL-1Ra–treatment group), 10 mg/kg (579.5 nmol/kg) anakinra in 200 μl of sterile saline (anakinra treatment group), or sterile saline alone (control group). These groups were then stimulated with MSU crystals and harvested as detailed in the previous experiment.

Cell counts

Leukocyte populations in mouse blood and i.p. fluid were evaluated using an automated cell counter (Heska® HemaTrue®, Loveland, CO). The i.p. fluid was centrifuged to pellet the cells (see above), which were resuspended in 500 μl of PBS for counting. Blood was diluted 1 part in 2 for counting.

Whole-blood culture

Blood removed at sacrifice was diluted 1 part in 5 in RPMI 1640 medium supplemented with 100 units/ml penicillin and 0.1 mg/ml streptomycin and seeded in 200-μl triplicate wells in round-bottom 96-well plates for spontaneous cytokine production. Cultures were incubated at 37 °C and 5% CO_2 for 24 h. Supernatants were centrifuged and aspirated for specific ELISA for mouse IL-6. Then, IL-6 levels were normalized by total WBC, as assessed by automated cell counter. For Fig. 5*G*, the mean IL-6 per WBC in the vehicle group was set at 100%, and then all points were expressed as percent of the vehicle mean.

A549 cell culture

A549 cells (ATCC, Manassas, VA) were cultured in 75-mm^2 flasks with F-12K media supplemented with 10% v/v FCS, 100 units/ml penicillin, and 0.1 mg/ml streptomycin at 37 °C under 5% CO_2. Media were refreshed every 3 days, and the culture was split at 70% confluence using 0.25% trypsin/EDTA.

A549 in vitro stimulation

5×10^4 cells per well were seeded in triplicate in round-bottom 96-well plates in complete F-12K media. Cells were pretreated with 579.5, 57.95, or 5.795 nM inhibitor (anakinra, PAS600–IL-1Ra, or PAS800–IL-1Ra) for 1 h. Then, 10 ng/ml recombinant human IL-1α was added, and the culture was incubated 24 h at 37 °C under 5% CO_2. Culture plates were centrifuged for 4 min at 244 $\times$ *g* at 23 °C, and supernatants were aspirated and analyzed for mouse IL-6 and IL-8 via specific ELISA. Then, the mean of the triplicate IL-1α–stimulated positive control wells was set as 100%, and the triplicate well averages of all other experimental conditions were then expressed as percent of the positive control mean.

PBMC isolation and culture

Healthy donor human peripheral venous blood was collected in vacuum tubes with EDTA added (BD Biosciences), and PBMCs were separated in a Histopaque®-1077 (Sigma) gradient with centrifugation and saline wash as per the manufacturer's instructions. Collected cells were counted using a hemocytometer, then centrifuged 4 min at 244 $\times$ *g* at 23 °C, and resuspended in complete RPMI 1640 medium. 10^5 cells per well were seeded in triplicate in round-bottom 96-well plates in 200 μl. Cells were pretreated with 579.5, 57.95, or 5.795 nM inhibitor (anakinra, PAS600–IL-1Ra, or PAS800–IL-1Ra) in RPMI medium for 1 h. Then, 5×10^4/ml heat-killed *C. albicans* were added, and the culture was incubated 5 days (120 h) at 37 °C under 5% CO_2. Supernatants were aspirated and analyzed for human IL-22 via specific ELISA. Then, the mean of the triplicate *C. albicans*–stimulated positive control wells was set as 100%, and the triplicate well averages of all other experimental conditions were then expressed as percent of the positive control mean.

Real-time SPR receptor-binding analysis of PAS–IL-1Ra fusion proteins

SPR spectroscopy was performed on a BIAcore 2000 instrument (GE Healthcare, Uppsala, Sweden). To investigate the influence of PASylation® on binding kinetics, a fusion protein (Symansis, Timaru, New Zealand) consisting of the extracellular domain of human IL-1 receptor I (IL-1RI) (aa 1–333) and the Fc region of human IgG1 (aa 93–330) was immobilized on a CM3 sensorchip (GE Healthcare) via an amine-coupled anti-human Fc antibody (Jackson ImmunoResearch, West Grove, PA) at 5 μg/ml in PBS, 0.05% Tween 20, resulting in a surface density of ~180 resonance units (ΔRU). In-house–produced PAS800–IL-1Ra (see supporting Experimental methods) and the drug anakinra (Swedish Orphan Biovitrum, Stockholm, Sweden) were diluted in 4 mM KH_2PO_4, 16 mM Na_2HPO_4, 115 mM NaCl, 0.05% (v/v) Tween® 20, pH 7.4 (PBS/T), and injected

in appropriate concentration series using PBS/T as running buffer. Complex formation was observed at a continuous flow rate of 25 μl/min, and the kinetic parameters were determined by fitting the data to the a 1:1 Langmuir binding model for bimolecular complex formation using BIAevaluation software version 4.1.1 (BIAcore). Sensorgrams were corrected by double subtraction of the corresponding signals measured for the in-line control blank channel and an averaged baseline determined from several buffer blank injections. To determine a reliable dissociation constant (k_{off}), complex dissociation was followed for 3600 s in the case of the two highest analyte concentrations. Chip regeneration was achieved with 10 mM glycine/HCl, pH 1.7.

Statistical analysis

Statistical significance was determined by two-tailed Student's *t* tests using GraphPad Prism version 8.0.1 for Macintosh (GraphPad Software, San Diego, CA).

Author contributions—N. E. P., C. M., D. M. d. G., U. B., C. K. E., A. S., and C. A. D. conceptualization; N. E. P., B. S., C. M., A. L., and M. S. data curation; N. E. P., B. S., C. M., D. M. d. G., R. D., U. B., C. K. E., A. S., and C. A. D. formal analysis; N. E. P., C. M., D. M. d. G., and C. A. D. supervision; N. E. P., B. S., A. L., M. S., U. B., and A. S. validation; N. E. P., A. L., M. S., U. B., C. K. E., A. S., and C. A. D. investigation; N. E. P., B. S., C. M., D. M. d. G., A. L., M. S., U. B., A. S., and C. A. D. methodology; N. E. P. and C. A. D. writing-original draft; N. E. P., B. S., R. D., U. B., C. K. E., A. S., and C. A. D. project administration; N. E. P., D. M. d. G., R. D., U. B., C. K. E., A. S., and C. A. D. writing-review and editing; A. L., M. S., R. D., U. B., and A. S. resources; A. L., M. S., U. B., and A. S. visualization; R. D., U. B., C. K. E., A. S., and C. A. D. funding acquisition.

Acknowledgments—We are grateful to Suzhao Li and Tania Azam for advice and technical support. We are also grateful to Klaus Wachinger for technical assistance and Tobias Kruse for contributions at an earlier stage of this project. XL-protein GmbH was recipient of Grant EP140440 from the German Bundesministerium für Wirtschaft und Energie.

References

1. Mantovani, A., Barajon, I., and Garlanda, C. (2018) IL-1 and IL-1 regulatory pathways in cancer progression and therapy. *Immunol. Rev.* **281,** 57–61 CrossRef Medline
2. Mantovani, A., Dinarello, C. A., Molgora, M., and Garlanda, C. (2019) Interleukin-1 and related cytokines in the regulation of inflammation and immunity. *Immunity* **50,** 778–795 CrossRef Medline
3. Rider, P., Carmi, Y., Guttman, O., Braiman, A., Cohen, I., Voronov, E., White, M. R., Dinarello, C. A., and Apte, R. N. (2011) IL-1α and IL-1β recruit different myeloid cells and promote different stages of sterile inflammation. *J. Immunol.* **187,** 4835–4843 CrossRef Medline
4. Van Opdenbosch, N., and Lamkanfi, M. (2019) Caspases in cell death, inflammation, and disease. *Immunity* **50,** 1352–1364 CrossRef Medline
5. Sobowale, O. A., Parry-Jones, A. R., Smith, C. J., Tyrrell, P. J., Rothwell, N. J., and Allan, S. M. (2016) Interleukin-1 in stroke: from bench to bedside. *Stroke* **47,** 2160–2167 CrossRef Medline
6. Marchetti, C., Toldo, S., Chojnacki, J., Mezzaroma, E., Liu, K., Salloum, F. N., Nordio, A., Carbone, S., Mauro, A. G., Das, A., Zalavadia, A. A., Halquist, M. S., Federici, M., Van Tassell, B. W., Zhang, S., and Abbate, A. (2015) Pharmacologic inhibition of the NLRP3 inflammasome preserves cardiac function after ischemic and nonischemic injury in the mouse. *J. Cardiovasc. Pharmacol.* **66,** 1–8 CrossRef Medline
7. Dinarello, C. A., Goldin, N. P., and Wolff, S. M. (1974) Demonstration and characterization of two distinct human leukocytic pyrogens. *J. Exp. Med.* **139,** 1369–1381 CrossRef Medline
8. Dayer, J.-M., Oliviero, F., and Punzi, L. (2017) A brief history of IL-1 and IL-1 Ra in rheumatology. *Front. Pharmacol.* **8,** 293 CrossRef Medline
9. Larsen, C. M., Faulenbach, M., Vaag, A., Vølund, A., Ehses, J. A., Seifert, B., Mandrup-Poulsen, T., and Donath, M. Y. (2007) Interleukin-1-receptor antagonist in type 2 diabetes mellitus. *N. Engl. J. Med.* **356,** 1517–1526 CrossRef Medline
10. Lane, T., Williams, R., Rowczenio, D., Youngstein, T., Trojer, H., Pepper, R., Brogan, P., Hawkins, P., and Lachmann, H. (2015) A decade of anti-IL-1 therapy in CAPS–a spectrum of efficacy in this spectrum of diseases. *Pediatr. Rheumatol. Online J.* **13,** O65 CrossRef
11. Szekely, Y., and Arbel, Y. (2018) A review of Interleukin-1 in heart disease: where do we stand today? *Cardiol. Ther.* **7,** 25–44 CrossRef Medline
12. Weber, A., Wasiliew, P., and Kracht, M. (2010) Interleukin-1 (IL-1) pathway. *Sci. Signal.* **3,** 1–7 CrossRef
13. Liu, T., Zhang, L., Joo, D., and Sun, S.-C. (2017) NF-κB signaling in inflammation. *Signal. Transduct. Tar. Ther.* **2,** 17023 CrossRef
14. Cavalli, G., and Dinarello, C. A. (2019) Anakinra therapy for non-cancer inflammatory diseases. *Front. Pharmacol.* **10,** 148 CrossRef Medline
15. Aksentijevich, I., Masters, S. L., Ferguson, P. J., Dancey, P., Frenkel, J., van Royen-Kerkhoff, A., Laxer, R., Tedgård, U., Cowen, E. W., Pham, T.-H., Booty, M., Estes, J. D., Sandler, N. G., Plass, N., Stone, D. L., et al. (2009) An autoinflammatory disease with deficiency of the interleukin-1–receptor antagonist. *N. Engl. J. Med.* **360,** 2426–2437 CrossRef Medline
16. Arend, W. P. (2002) The balance between IL-1 and IL-1Ra in disease. *Cytokine Growth Factor Rev.* **13,** 323–340 CrossRef Medline
17. Fleischmann, R., Stern, R., and Iqbal, I. (2004) Anakinra: an inhibitor of IL-1 for the treatment of rheumatoid arthritis. *Expert Opin. Biol. Ther.* **4,** 1333–1344 CrossRef Medline
18. Campion, G. V., Lebsack, M. E., Lookabaugh, J., Gordon, G., and Catalano, M. (1996) Dose-range and dose-frequency study of recombinant human interleukin-1 receptor antagonist in patients with rheumatoid arthritis. *Arthritis Rheum.* **39,** 1092–1101 CrossRef Medline
19. Cohen, S., Hurd, E., Cush, J., Schiff, M., Weinblatt, M. E., Moreland, L. W., Kremer, J., Bear, M. B., Rich, W. J., and McCabe, D. (2002) Treatment of rheumatoid arthritis with anakinra, a recombinant human interleukin-1 receptor antagonist, in combination with methrotrexate: results of a twenty-four-week, multicenter, randomized, double-blind, placebo-controlled trial. *Arthritis Rheum.* **46,** 614–624 CrossRef Medline
20. Ortiz-Sanjuán, F., Blanco, R., Riancho-Zarrabeitia, L., Castañeda, S., Olivé, A., Riveros, A., Velloso-Feijoo, M. L., Narváez, J., Jiménez-Moleón, I., Maiz-Alonso, O., Ordóñez, C., Bernal, J. A., Hernández, M. V., Sifuentes-Giraldo, W. A., Gómez-Arango, C., *et al.* (2015) Efficacy of anakinra in refractory adult-onset Still's disease: multicenter study of 41 patients and literature review. *Medicine* **94,** e1554 CrossRef Medline
21. Grevich, S., and Shenoi, S. (2017) Update on the management of systemic juvenile idiopathic arthritis and role of IL-1 and IL-6 inhibition. *Adolesc. Health Med. Ther.* **8,** 125–135 CrossRef Medline
22. Aouba, A., Deshayes, S., Frenzel, L., Decottignies, A., Prussia, C., Bienvenu, B., Boue, F., Damaj, G., Hermine, O., and Georgin-Lavialle, S. (2015) Efficacy of anakinra for various types of crystal-induced arthritis in complex hospitalized patients: a case series and review of the literature. *Mediators. Inflamm.* **2015,** 792173 CrossRef Medline
23. Diakos, C. I., Charles, K. A., McMillan, D. C., and Clarke, S. J. (2014) Cancer-related inflammation and treatment effectiveness. *Lancet Oncol.* **15,** e493–e503 CrossRef Medline
24. Xie, R., Zhang, Y., Zhao, N., Zhou, S., Wang, X., Han, W., Yu, Y., Zhao, X., and Cui, Y. (2019) Pharmacokinetics and safety of recombinant human interleukin-1 receptor antagonist GR007 in healthy Chinese subjects. *Eur. J. Drug Metab. Pharmacokinet.* **44,** 353–360 CrossRef Medline
25. Holt, L. J., Basran, A., Jones, K., Chorlton, J., Jespers, L. S., Brewis, N. D., and Tomlinson, I. M. (2008) Anti-serum albumin domain antibodies for extending the half-lives of short-lived drugs. *Protein Eng. Des. Sel.* **21,** 283–288 CrossRef Medline
26. Schiff, M., Saunderson, S., Mountian, I., and Hartley, P. (2017) Chronic disease and self-injection: ethnographic investigations into the patient

experience during treatment. *Rheumatol. Ther.* **4,** 445–463 CrossRef Medline
27. Schlapschy, M., Binder, U., Börger, C., Theobald, I., Wachinger, K., Kisling, S., Haller, D., and Skerra, A. (2013) PASylation: a biological alternative to PEGylation for extending the plasma half-life of pharmaceutically active proteins. *Protein Eng. Des. Sel.* **26,** 489–501 CrossRef Medline
28. Di Cesare, S., Binder, U., Maier, T., and Skerra, A. (2013) High-yield production of PASylated human growth hormone using secretory *E. coli* technology. *BioProcess Int.* **11,** 30–38.
29. Xia, Y., Schlapschy, M., Morath, V., Roeder, N., Vogt, E. I., Stadler, D., Cheng, X., Dittmer, U., Sutter, K., Heikenwalder, M., Skerra, A., and Protzer, U. (2019) PASylated interferon α efficiently suppresses hepatitis B virus and induces anti-HBs seroconversion in HBV-transgenic mice. *Antiviral Res.* **161,** 134–143 CrossRef Medline
30. Morath, V., Bolze, F., Schlapschy, M., Schneider, S., Sedlmayer, F., Seyfarth, K., Klingenspor, M., and Skerra, A. (2015) PASylation of murine leptin leads to extended plasma half-life and enhanced *in vivo* efficacy. *Mol. Pharm.* **12,** 1431–1442 CrossRef Medline
31. Kuhn, N., Schmidt, C. Q., Schlapschy, M., and Skerra, A. (2016) PASylated Coversin, a C5-specific complement inhibitor with extended pharmacokinetics, shows enhanced anti-hemolytic activity *in vitro*. *Bioconjug. Chem.* **27,** 2359–2371 CrossRef Medline
32. Harari, D., Kuhn, N., Abramovich, R., Sasson, K., Zozulya, A. L., Smith, P., Schlapschy, M., Aharoni, R., Köster, M., Eilam, R., Skerra, A., and Schreiber, G. (2014) Enhanced *in vivo* efficacy of a type I interferon superagonist with extended plasma half-life in a mouse model of multiple sclerosis. *J. Biol. Chem.* **289,** 29014–29029 CrossRef Medline
33. Mendler, C. T., Friedrich, L., Laitinen, I., Schlapschy, M., Schwaiger, M., Wester, H.-J., and Skerra, A. (2015) High contrast tumor imaging with radio-labeled antibody Fab fragments tailored for optimized pharmacokinetics via PASylation. *MAbs* **7,** 96–109 CrossRef Medline
34. Gebauer, M., and Skerra, A. (2018) Prospects of PASylation® for the design of protein and peptide therapeutics with extended half-life and enhanced action. *Bioorg. Med. Chem.* **26,** 2882–2887 CrossRef Medline
35. Binder, U., and Skerra, A. (2017) PASylation®: a versatile technology to extend drug delivery. *Curr. Opin. Colloid Interface Sci.* **31,** 10–17 CrossRef
36. Nganou-Makamdop, K., Billingsley, J. M., Yaffe, Z., O'Connor, G., Tharp, G. K., Ransier, A., Laboune, F., Matus-Nicodemos, R., Lerner, A., Gharu, L., Robertson, J. M., Ford, M. L., Schlapschy, M., Kuhn, N., Lensch, A., *et al.* (2018) Type I IFN signaling blockade by a PASylated antagonist during chronic SIV infection suppresses specific inflammatory pathways but does not alter T cell activation or virus replication. *PLOS Pathog.* **14,** e1007246 CrossRef Medline
37. Rudmann, D. G., Alston, J. T., Hanson, J. C., and Heidel, S. (2013) High molecular weight polyethylene glycol cellular distribution and PEG-associated cytoplasmic vacuolation is molecular weight dependent and does not require conjugation to proteins. *Toxicol. Pathol.* **41,** 970–983 CrossRef Medline
38. Strohl, W. R. (2015) Fusion proteins for half-life extension of biologics as a strategy to make biobetters. *BioDrugs* **29,** 215–239 CrossRef Medline
39. Bendele, A., Seely, J., Richey, C., Sennello, G., and Shopp, G. (1998) Short communication: renal tubular vacuolation in animals treated with polyethylene glycol-conjugated proteins. *Toxicol. Sci.* **42,** 152–157 CrossRef Medline
40. Breibeck, J., and Skerra, A. (2018) The polypeptide biophysics of proline/alanine-rich sequences (PAS): recombinant biopolymers with PEG-like properties. *Biopolymers* **109,** e23069 CrossRef Medline
41. Mitragotri, S., Burke, P. A., and Langer, R. (2014) Overcoming the challenges in administering biopharmaceuticals: formulation an delivery strategies. *Nat. Rev. Drug Discov.* **13,** 655–672 CrossRef Medline
42. Mahmood, I. (2004) Interspecies scaling of protein drugs: prediction of clearance from animals to humans. *J. Pharm. Sci.* **93,** 177–185 CrossRef Medline
43. So, A., De Smedt, T., Revaz, S., and Tschopp, J. (2007) A pilot study of IL-1 inhibition by anakinra in acute gout. *Arthritis Res. Ther.* **9,** R28 CrossRef Medline
44. Cromwell, O., Hamid, Q., Corrigan, C. J., Barkans, J., Meng, Q., Collins, P. D., and Kay, A. B. (1992) Expression and generation of interleukin-8, IL-6 and granulocyte-macrophage colony-stimulating factor by bronchial epithelial cells and enhancement by IL-1β and tumor necrosis factor-α. *Immunology* **77,** 330–337 Medline
45. Markota, A., Endres, S., and Kobold, S. (2018) Targeting interleukin-22 for cancer therapy. *Hum. Vaccin. Immunother.* **14,** 2012–2015 CrossRef Medline
46. Vermeire, E., Hearnshaw, H., Van Royen, P., and Denekens, J. (2001) Patient adherence to treatment: three decades of research. A comprehensive review. *J. Clin. Pharm. Ther.* **26,** 331–342 CrossRef Medline
47. Perez-Ruiz, F., and Desideri, G. (2018) Improving adherence to gout therapy: an expert review. *Ther. Clin. Risk Manag.* **14,** 793–802 CrossRef Medline
48. Busso, N., and So, A. (2010) Mechanisms of inflammation in gout. *Arthritis Res. Ther.* **12,** 206 CrossRef Medline
49. Harrold, L. R., Mazor, K. M., Velten, S., Ockene, I. S., and Yood, R. A. (2010) Patients and providers view gout differently: a qualitative study. *Chronic Illn.* **6,** 263–271 CrossRef Medline
50. Dinarello, C. A. (2019) The IL-1 family of cytokines and receptors in rheumatic diseases. *Nat. Rev. Rheumatol.* **15,** 612–632 CrossRef Medline
51. Ridker, P. M., Everett, B. M., Thuren, T., MacFadyen, J. G., Chang, W. H., Ballantyne, C., Fonseca, F., Nicolau, J., Koenig, W., Anker, S. D., Kastelein, J. J. P., Cornel, J. H., Pais, P., Pella, D., Genest, J., *et al.* (2017) Antiinflammatory therapy with canakinumab for atherosclerotic disease. *N. Engl. J. Med.* **377,** 1119–1131 CrossRef Medline
52. Everett, B. M., Donath, M. Y., Pradhan, A. D., Thuren, T., Pais, P., Nicolau, J. C., Glynn, R. J., Libby, P., and Ridker, P. M. (2018) Anti-inflammatory therapy with Canakinumab for the prevention and management of diabetes. *J. Am. Coll. Cardiol.* **71,** 2392–2401 CrossRef Medline
53. Ruscitti, P., Masedu, F., Alvaro, S., Airò, P., Battafarano, N., Cantarini, L., Cantatore, F. P., Carlino, G., D'Abrosca, V., Frassi, M., Frediani, B., Iacono, D., Liakouli, V., Maggio, R., Mulè, R., *et al.* (2019) Anti-interleukin-1 treatment in patients with rheumatoid arthritis and type 2 diabetes (TRACK): A multicentre, open-label, randomised controlled trial. *PLoS Med.* **16,** e1002901 CrossRef Medline
54. Everett, B. M., Cornel, J. H., Lainscak, M., Anker, S. D., Abbate, A., Thuren, T., Libby, P., Glynn, R. J., and Ridker, P. M. (2019) Anti-inflammatory therapy with canakinumab for the prevention of hospitalization for heart failure. *Circulation* **139,** 1289–1299 CrossRef Medline
55. Abbate, A., Van Tassell, B. W., Biondi-Zoccai, G., Kontos, M. C., Grizzard, J. D., Spillman, D. W., Oddi, C., Roberts, C. S., Melchior, R. D., Mueller, G. H., Abouzaki, N. A., Rengel, L. R., Varma, A., Gambill, M. L., Falcao, R. A., *et al.* (2013) Effects of interleukin-1 blockade with anakinra on adverse cardiac remodeling and heart failure after acute myocardial infarction (from the Virginia Commonwealth University–Anakinra Remodeling Trial (2) (VCU-ART2) pilot study). *Am. J. Cardiol.* **111,** 1394–1400 CrossRef Medline
56. Dudakov, J. A., Hanash, A. M., and van den Brink, M. R. (2015) Interleukin-22: immunobiology and pathology. *Annu. Rev. Immunol.* **33,** 747–785 CrossRef Medline
57. Ridker, P. M., MacFadyen, J. G., Thuren, T., Everett, B. M., Libby, P., Glynn, R. J., and CANTOS Trial Group. (2017) Effect of interleukin-1β inhibition with canakinumab on incident lung cancer in patients with atherosclerosis: exploratory results from a randomised, double-blind, placebo-controlled trial. *Lancet* **390,** 1833–1842 CrossRef Medline
58. Kubetzko, S., Sarkar, C. A., and Plückthun, A. (2005) Protein PEGylation decreases observed target association rates via a dual blocking mechanism. *Mol. Pharmacol.* **68,** 1439–1454 CrossRef Medline
59. Längin, M., Mayr, T., Reichart, B., Michel, S., Buchholz, S., Guethoff, S., Dashkevich, A., Baehr, A., Egerer, S., Bauer, A., Mihalj, M., Panelli, A., Issl, L., Ying, J., Fresch, A. K., *et al.* (2018) Consistent success in life-supporting porcine cardiac xenotransplantation. *Nature* **564,** 430–433 CrossRef Medline
60. Griffiths, K., Binder, U., McDowell, W., Tommasi, R., Frigerio, M., Darby, W. G., Hosking, C. G., Renaud, L., Machacek, M., Lloyd, P., Skerra, A., and Foley, M. (2019) Half-life extension and non-human primate pharmaco-

kinetic safety studies of i-body AD-114 targeting human CXCR4. *MAbs* **11,** 1331–1340 CrossRef Medline
61. Fleischmann, R. M., Tesser, J., Schiff, M. H., Schechtman, J., Burmester, G.-R., Bennett, R., Modafferi, D., Zhou, L., Bell, D., and Appleton, B. (2006) Safety of extended treatment with anakinra in patients with rheumatoid arthritis. *Ann. Rheum. Dis.* **65,** 1006–1012 CrossRef Medline
62. Ramírez, J., and Cañete, J. D. (2018) Anakinra for the treatment of rheumatoid arthritis: a safety evaluation. *Expert Opin. Drug Saf.* **17,** 727–732 CrossRef Medline
63. Doeleman, M. J. H., van Maarseveen, E. M., and Swart, J. F. (2019) Immunogenicity of biologic agents in juvenile idiopathic arthritis: a systemic review and meta-analysis. *Rheumatology* 58, 1839–1849 CrossRef Medline
64. Hermeling, S., Crommelin, D. J., Schellekens, H., and Jiskoot, W. (2004) Structure-immunogenicity relationships of therapeutic proteins. *Pharm. Res.* **21,** 897–903 CrossRef Medline
65. Baker, M. P., Reynolds, H. M., Lumicisi, B., and Bryson, C. J. (2010) Immunogenicity of protein therapeutics: the key causes, consequences and challenges. *Self Nonself* **1,** 314–322 CrossRef Medline
66. Wadhwa, M., Knezevic, I., Kang, H.-N., and Thorpe, R. (2015) Immunogenicity assessment of biotherapeutic products: an overview of assays and their utility. *Biologicals* **43,** 298–306 CrossRef Medline
67. Schreuder, H., Tardif, C., Trump-Kallmeyer, S., Soffientini, A., Sarubbi, E., Akeson, A., Bowlin, T., Yanofsky, S., and Barrett, R. W. (1997) A new cytokine-receptor binding mode revealed by the crystal structure of the IL-1 receptor with an antagonist. *Nature* **386,** 194–200 CrossRef Medline